

# MONTE CARLO PERFORMANCE BENCHMARK FOR DETAILED POWER DENSITY CALCULATION IN A FULL SIZE REACTOR CORE

## *Benchmark specifications* Revision 1.2, July 2011

**J. Eduard Hoogenboom**  
Faculty of Applied Sciences  
Delft University of Technology  
Mekelweg 15,  
2629 JB Delft,  
The Netherlands  
j.e.hoogenboom@tudelft.nl

**William R. Martin**  
Nuclear Engineering and  
Radiological Sciences  
University of Michigan  
Ann Arbor, MI 48109-2104,  
USA  
wrm@umich.edu

**Bojan Petrovic**  
Nuclear and Radiological  
Engineering  
Georgia Institute of Technology  
Atlanta, GA 30332-0405,  
USA  
Bojan.Petrovic@gatech.edu

## 1. Introduction

Monte Carlo codes are capable of calculating integral parameters such as the effective multiplication factor or a reactivity coefficient, allowing all geometrical details of each individual fuel pin of each fuel assembly to be modeled. However, when more detailed information is required such as local power densities for a large number of small regions of a fuel pin, it is much more difficult to get reliable results with respect to the associated statistical uncertainty (typically represented by its standard deviation) within an acceptable computation time. Nonetheless, this is the requirement for current design calculations of a nuclear reactor core.

In his invited lecture at the M&C 2003 conference in Gatlinburg, Kord Smith [1] formulated the challenge for future Monte Carlo simulation as the calculation of the local power of each of the fuel pins in a fuel assembly when subdivided in 100 axial and 10 radial zones for burnup calculations. The number of fuel pins in a typical fuel assembly of a PWR core is between 200 and 300 while the number of fuel assemblies in a reactor core is around 200. This results in the total of perhaps 40-60 million tallies. For an acceptable result, Smith specified that the standard deviation in each local power region should be 1 % or less. In addition, Smith considered 100 different nuclides for which the reaction rate is needed, bringing the total number of tallies to 6 billion. This huge number of tallies not only poses a problem in CPU time but also in computer memory. Smith estimated on the basis of Moore's law that it will be 2030 before such a full core Monte Carlo calculation could be done in less than one hour on a single CPU.

Bill Martin [2] analyzed the situation in some detail in his invited lecture at the M&C 2007 conference in Monterey. Assuming that Moore's law manifests itself as *only* more cores in a desktop computer, Martin estimated that it would be 2019 before a full reactor core calculation with 40,000 fuel pins and 100 axial regions and 1 % statistical accuracy for local power

estimates could be accomplished in one hour calculation time. In this case, the desktop computer would have a 1500 core processor at that time.

There are several reasons why the advances in efficiency of full core Monte Carlo reactor calculations may be better or worse than estimated above. No improvements in single processor speed has been taken into account, nor advances in other types of processing units. In addition, no progress in Monte Carlo variance reduction techniques is assumed. On the other hand, it is not guaranteed that Moore's law, in whatever form, will continue to hold over a period of 10 years, although it did hold over a longer period in the past. In fact, some computer design experts believe that the heat dissipation requirement will present a fundamental limit to the sustained increase of computational power. Moreover, the performance of a Monte Carlo calculation will not scale linearly with the number of cores in a processor, due to the communication overhead and/or decomposition of the problem. Also, the handling of very large numbers of tallies will further slow down the Monte Carlo calculation.

For all these reasons it will be useful to monitor the performance of Monte Carlo full core calculations over the next 1 or 2 decades to assess the progress towards meeting the "Kord Smith challenge". Therefore, a suitable benchmark test which exhibits sufficient realistic detail for a modern full core calculation is needed.

## **2. Specific aim of the benchmark test**

The aim of the proposed benchmark test is to monitor over the coming years the (increase in) performance of Monte Carlo calculations of a full size reactor core. To address the above mentioned issues, the key quantity to be estimated is not the effective multiplication factor, but the local power densities, and possibly reaction rates, in small regions of the fuel. Moreover, the value of the power density itself is not the most important quantity, although it should be estimated correctly, but rather its standard deviation in relation to the number of neutron histories and computing time. In this respect the total number of tallies, i.e. the total number of fuel regions for which the power density is calculated, is relevant for the execution time. On the other hand, the number of tallies may be restricted by the Monte Carlo code used and/or the available computer memory. Hence, besides the power density of a number of specifically denoted fuel regions spread over the full core and their standard deviation, the number of other tallies used in the calculation, without quoting their specific results, is a parameter which should be chosen as large as reasonably possible, ultimately aiming to the previously mentioned 6 billion tallies.

In addition to the number of neutron histories simulated (as a product of the nominal number of histories per cycle and the number of active cycles) and the resulting standard deviation in the power density at specific fuel volumes, the computing time is, of course, an important measure in this benchmark. Considering the use of computer systems with many nodes and/or a number of cores per node, the wall clock time for execution of a full Monte Carlo run is a target quantity. For extrapolation to a very large number of cores in the future, the speedup as a function of the number of cores is also important. The capacity of computer systems will change over the years, but that is what we want to monitor.

In view of the specific aim of this benchmark to measure the computational performance of a full-core Monte Carlo simulation, issues such as fission source convergence, while important for practical application of Monte Carlo reactor calculations, are not part of this benchmark at this stage, but may be addressed in future extended versions. Therefore, we propose to look only at active cycles for which source convergence is already achieved, no matter what it takes to reach that state. Moreover, we will not consider reactivity feedbacks (e.g., temperature dependence) or evolution of burnup. To avoid inconsistencies in this respect, the fuel compositions in terms of nuclide densities and temperatures are explicitly defined. There will be, of course, differences in outcome of the local power densities due to differences in nuclear data, but such differences are not the subject of this benchmark, rather it is the efficiency of the calculation that is being measured.

A secondary aim of the benchmark test is to stimulate improvements in Monte Carlo codes and their implementation. This not only refers to improving the efficiency of generating random walks of neutrons in a full core nuclear reactor, but also to improving methods for dealing with large numbers of tallies (i.e., local power densities in many small fuel regions) and various issues in high performance computing like efficiency improvements in parallel computing using current and future computer architectures generally available to researchers and engineers. Another issue is the quality of the high performance programming of the Monte Carlo code and the performance of the compiler. All these items are implicitly part of the benchmark test.

### **3. Benchmark specifications**

For the geometry and composition of the reactor core we took a large PWR core as a reference without trying to model any specific existing reactor. As the aim of the proposed benchmark test is not to get detailed information about one specific reactor core, the details of the geometry and composition of the reactor core and fuel assemblies are not critical, as long as they require the Monte Carlo code to do realistic neutron history simulation with most of the features encountered in current reactor design. Therefore, a number of simplifications are made in geometry and composition of materials.

#### **3.1 Core configuration**

The core consists of 241 identical fuel assemblies with arrangement shown in Fig. 1. The dimensions of a fuel assembly are  $21.42 \times 21.42 \text{ cm}^2$ . In an actual PWR, the core is typically bounded by baffle plates, followed by the so-called former region (mostly borated water plus some steel plates), core barrel, and downcomer (borated water). In this simplified model, the first three regions have been homogenized into a radial reflector region. The downcomer with cold (borated) water forms a cylindrical shell with inner radius 209 cm and outer radius 229 cm. The reactor vessel has an outer radius of 249 cm.

Fig. 2 shows a vertical cross section of the reactor core. The active fuel length is 366 cm. To introduce an asymmetry in the vertical direction and to model in an approximate way the decreasing coolant density from bottom to top the water density in a fuel assembly and in the radial reflector is higher below the core midplane and lower above the core midplane (see Sect.

3.2 for actual composition specifications). Therefore, different colors are used in Fig. 2 for the zones below and above the core midplane.

Above the active fuel zone a homogeneous top fuel assembly region represents the upper plenum in the fuel rods, the rod end-plug, the grid plate and the water space to the top nozzle. This region is 20 cm high. Above this region a homogeneous top nozzle region of 12 cm height and above that the upper core plate region of 8 cm height are both modeled. If the core midplane is assumed at  $z=0$  then the maximum  $z$ -value becomes  $z = 183+20+8+12 = 223$  cm. The reactor vessel is also modeled up to this height.

Below the active fuel zone is a homogenized bottom fuel assembly region that models the lower rod end-plug, the grid plate and the water space to the bottom nozzle of 10 cm height. Below this region a homogenized bottom nozzle region of 6 cm height and below that the lower core plate region of 30 cm height are modeled. The minimum  $z$ -value from the core midplane becomes  $z = -183-10-6-30 = -229$  cm. The downcomer extends over the active fuel zone, the top and bottom fuel assembly regions and the top and bottom nozzle regions, hence from  $z = -199$  cm to  $z = +215$  cm. To simplify the modeling of the top and bottom fuel assembly and nozzle regions, these regions are represented as cylindrical volumes with an effective radius of 187.6 cm, which preserves the cross sectional area of the 241 fuel assemblies.

The radial and upper/lower axial reflector regions, as defined, provide a reasonably realistic representation of a PWR non-fuel region that would need to be modeled in order to obtain a realistic simulation.

Vacuum (i.e., non-re-entrant) boundary conditions are assumed above and below the core system and outside the pressure vessel.

Although the core lay-out as defined here shows symmetry in the  $x$ - $y$  plane, *it is the explicit intention and requirement to model the full core and not take possible advantage of any symmetry in the geometry.*

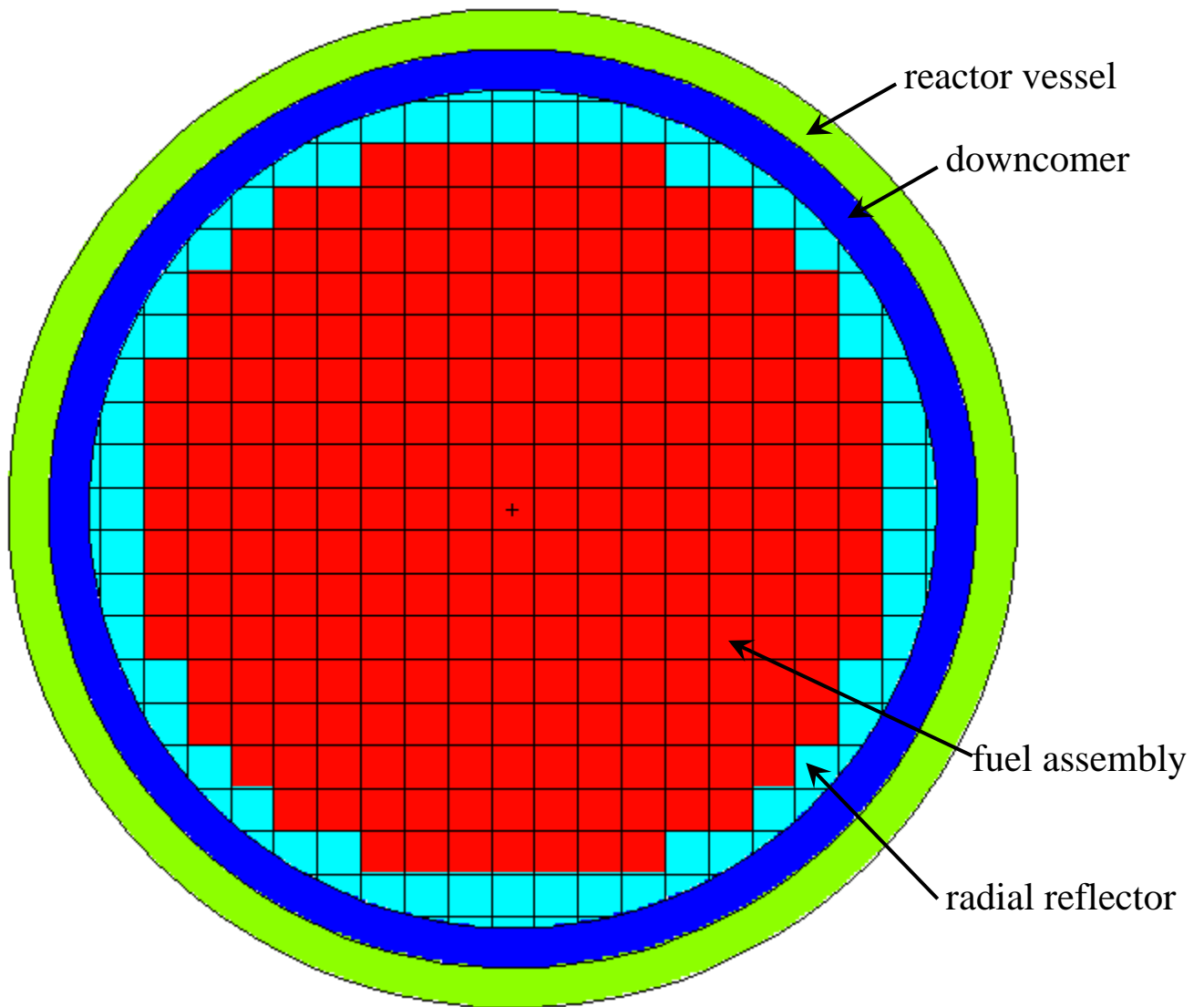


Fig. 1 Horizontal cross section of reactor core with fuel assemblies

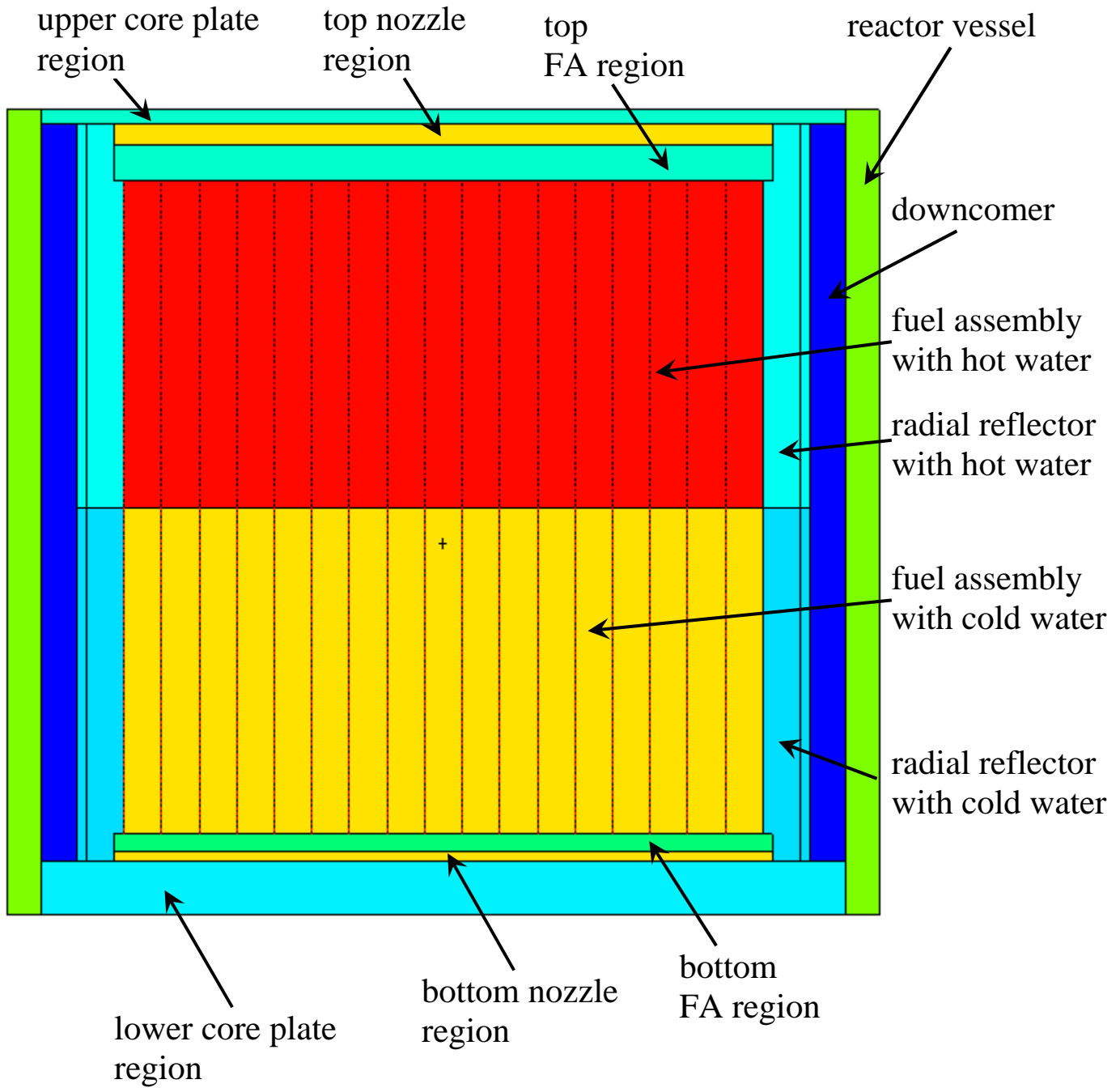


Fig. 2. Vertical cross section of reactor core with pressure vessel

### 3.2 Fuel assembly configuration

Each fuel assembly consists of 17 x 17 unit cells as shown in Fig. 3. The dimension of the unit cell is 1.26 x 1.26 cm<sup>2</sup>, making up the outer dimensions of the fuel assembly of 17 x 1.26 cm = 21.42 cm. No spacers or other construction material for an assembly are modeled. No intra-assembly gap is assumed.

Out of 289 lattice locations, 24 symmetrically positioned unit cells are occupied by control rod instrumentation guide tubes, and the central location is filled with an instrumentation tube. No inserted control rods are modeled; thus, the guide tubes are filled with water. The inner radius of a guide tube is 0.56 cm, and the outer radius is 0.62 cm. The instrumentation tube is effectively identical to a guide tube.

At the other unit cell positions fuel pins with cladding are present. Each fuel pin has an outer radius of 0.41 cm. The cladding has an outer radius of 0.475 cm. No gap is modeled.

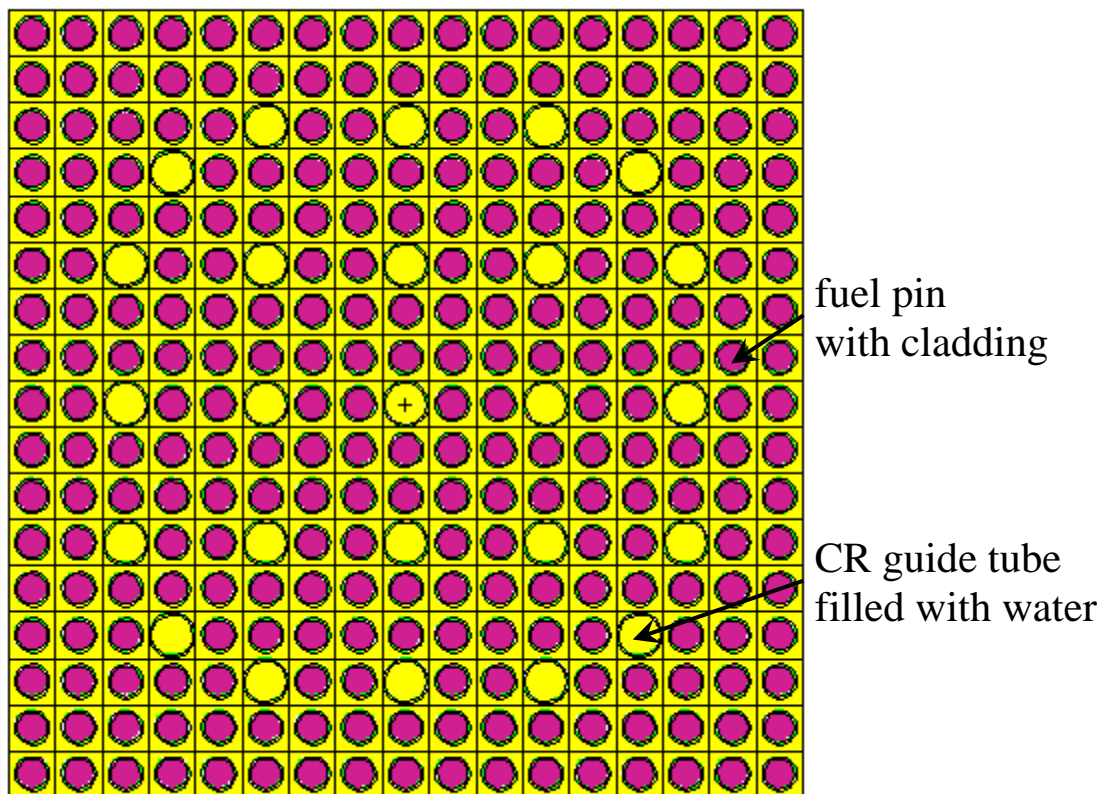


Fig. 3. Horizontal cross section of a fuel assembly

### 3.3 Material composition

#### 3.3.1 Fuel composition

The effort in sampling the cross section value depends on the number of nuclides at the interaction site. In order to take into account a reasonable number of nuclides in the fuel, the fuel composition is taken at a certain burnup stage (roughly 24,000 MWd/ton) from which 17 actinides are selected together with 16 fission products, and oxygen. Table I shows the composition of the fuel in terms of atom densities. The total atom density is  $0.06822 \times 10^{24} \text{ cm}^{-3}$  resulting in a mass density of  $10.062 \text{ g/cm}^3$ .

**Table I. UOX fuel composition**

nuclide	atom density x $10^{-24} \text{ cm}^{-3}$	nuclide	atom density x $10^{-24} \text{ cm}^{-3}$
$^{234}_{92}\text{U}$	$4.9476 \times 10^{-6}$	$^{95}_{42}\text{Mb}$	$2.6497 \times 10^{-5}$
$^{235}_{92}\text{U}$	$4.8218 \times 10^{-4}$	$^{99}_{43}\text{Tc}$	$3.2772 \times 10^{-5}$
$^{236}_{92}\text{U}$	$9.0402 \times 10^{-5}$	$^{101}_{44}\text{Ru}$	$3.0742 \times 10^{-5}$
$^{238}_{92}\text{U}$	$2.1504 \times 10^{-2}$	$^{103}_{44}\text{Ru}$	$2.3505 \times 10^{-6}$
$^{237}_{93}\text{Np}$	$7.3733 \times 10^{-6}$	$^{109}_{47}\text{Ag}$	$2.0009 \times 10^{-6}$
$^{238}_{94}\text{Pu}$	$1.5148 \times 10^{-6}$	$^{135}_{54}\text{Xe}$	$1.0801 \times 10^{-8}$
$^{239}_{94}\text{Pu}$	$1.3955 \times 10^{-4}$	$^{133}_{55}\text{Cs}$	$3.4612 \times 10^{-5}$
$^{240}_{94}\text{Pu}$	$3.4405 \times 10^{-5}$	$^{143}_{60}\text{Nd}$	$2.6078 \times 10^{-5}$
$^{241}_{94}\text{Pu}$	$2.1439 \times 10^{-5}$	$^{145}_{60}\text{Nd}$	$1.9898 \times 10^{-5}$
$^{242}_{94}\text{Pu}$	$3.7422 \times 10^{-6}$	$^{147}_{62}\text{Sm}$	$1.6128 \times 10^{-6}$
$^{241}_{95}\text{Am}$	$4.5041 \times 10^{-7}$	$^{149}_{62}\text{Sm}$	$1.1627 \times 10^{-7}$
$^{242}_{95}\text{Am}$	$9.2301 \times 10^{-9}$	$^{150}_{62}\text{Sm}$	$7.1727 \times 10^{-6}$
$^{243}_{95}\text{Am}$	$4.7878 \times 10^{-7}$	$^{151}_{62}\text{Sm}$	$5.4947 \times 10^{-7}$
$^{242}_{96}\text{Cm}$	$1.0485 \times 10^{-7}$	$^{152}_{62}\text{Sm}$	$3.0221 \times 10^{-6}$
$^{243}_{96}\text{Cm}$	$1.4268 \times 10^{-9}$	$^{153}_{63}\text{Eu}$	$2.6209 \times 10^{-6}$
$^{244}_{96}\text{Cm}$	$8.8756 \times 10^{-8}$	$^{155}_{64}\text{Gd}$	$1.5369 \times 10^{-9}$
$^{245}_{96}\text{Cm}$	$3.5285 \times 10^{-9}$	$^{16}_{8}\text{O}$	$4.5737 \times 10^{-2}$
Total atom density ( $\text{cm}^{-3}$ )		$0.06822 \times 10^{24}$	
Total mass density ( $\text{g/cm}^3$ )		10.062	

#### 3.3.2 Cladding composition

For convenience the cladding material is taken as (natural) zirconium. As the gap is not modeled, the cladding is smeared with the gap and the mass density of zirconium becomes

5.77 g/cm<sup>3</sup>. See Appendix A for the isotopic composition of Zr in case one is able to take into account all separate isotopes.

### 3.3.3 Borated water composition

The coolant is water and is present at two different densities, 0.74 g/cm<sup>3</sup> below the axial core midplane to represent “cold” water and 0.66 g/cm<sup>3</sup> above the core midplane to represent “hot” water. Boron is added to the coolant and its concentration is chosen such that the reactor is near critical. Boron is composed of 19.9 % <sup>10</sup>B and 80.1 % <sup>11</sup>B by atoms, which means 18.43 % <sup>10</sup>B and 81.57 % <sup>11</sup>B by weight fraction. Table II shows the atom fractions of the coolant nuclides relative to the water molecule fraction. Hence the total atom fraction is not normalized to unity.

For water with density 0.74 g/cm<sup>3</sup> the water molecule density, equal to the oxygen atom density, is 0.02469 10<sup>24</sup> cm<sup>-3</sup>. For a mass density of 0.66 g/cm<sup>3</sup> the water molecule density is 0.02202 10<sup>24</sup> cm<sup>-3</sup>. The total atom densities are given in Table II.

The coolant appears in the fuel assembly outside the fuel pin and cladding and inside and outside the guide tubes. It also appears in the downcomer, where its density over the full height of the system is 0.74 g/cm<sup>3</sup>.

In the regions below and above the core the water regions are smeared with the construction materials and the material composition of these regions is detailed in Sect. 3.3.5.

**Table II. Nuclide relative atom fraction of borated water**

nuclide	relative atom fraction
<sup>1</sup> <sub>1</sub> H	2
<sup>16</sup> <sub>8</sub> O	1
<sup>10</sup> <sub>5</sub> B	6.490 10 <sup>-4</sup>
<sup>11</sup> <sub>5</sub> B	2.689 10 <sup>-3</sup>
Total mass density (g/cm <sup>3</sup> )	0.74 (cold water) 0.66 (hot water)
Total atom density (cm <sup>-3</sup> )	0.07416 10 <sup>24</sup> (cold water) 0.06614 10 <sup>24</sup> (hot water)

### 3.3.4 Reactor pressure vessel composition

The pressure vessel material is modeled as low-carbon steel SA 508, grade 2. Its composition is specified in Table III, as well as the total mass density. For components with weight fraction less than 0.2 %, iron is substituted. As several of the elements are composed of various isotopes, the table in Appendix A provides the composition per element. The weight percentages from this table must be multiplied by the weight fraction

for the element from Table III to get the weight fraction per nuclide (as far as separate isotopes of an element can be taken into account).

**Table III. Composition of reactor pressure vessel material**

<b>element</b>	<b>weight percentage</b>
Fe	96.3
Ni	1.0
Mn	1.0
Mo	0.6
Si	0.4
Cr	0.25
C	0.25
Cu	0.2
Total mass density (g/cm <sup>3</sup> )	7.9

### 3.3.5 Homogenized water and stainless steel region composition

As described in Sect. 3.1 there are several regions for which the reactor construction is not detailed and in the benchmark geometry the construction (structural) material, assumed to be SS304, is smeared with the cooling water. As both the water density and the volume fraction of water can be different, Table IV specifies the compositions with reference to Fig. 2 to show where these regions are located.

Note that the upper radial reflector and the top plate region have the same composition.

See Appendix A for the isotopic composition of the structural elements (in case separate isotopes of an element can be taken into account).

**Table IV. Weight fraction per nuclide of smeared material**

<b>component</b>	<b>lower radial reflector</b>	<b>upper radial reflector</b>	<b>Bottom plate region</b>	<b>bottom nozzle region</b>	<b>top nozzle region</b>	<b>top plate region</b>
water density	0.74	0.66	0.74	0.74	0.66	0.66
water volume fraction	0.50	0.50	0.10	0.75	0.85	0.50
SS volume fraction	0.50	0.50	0.90	0.25	0.15	0.50
<b>Av. Density (g/cm<sup>3</sup>)</b>	<b>4.32</b>	<b>4.28</b>	<b>7.184</b>	<b>2.53</b>	<b>1.746</b>	<b>4.28</b>
<b>nuclide/elm.</b>	<b>weight fraction</b>					
<sup>1</sup> <sub>1</sub> H	0.0095661	0.0086117	0.0011505	0.0245014	0.0358870	0.0086117
<sup>16</sup> <sub>8</sub> O	0.0759107	0.0683369	0.0091296	0.1944274	0.2847761	0.0683369
<sup>10</sup> <sub>5</sub> B	3.08409 10 <sup>-5</sup>	2.77638 10 <sup>-5</sup>	3.70915 10 <sup>-6</sup>	7.89917 10 <sup>-5</sup>	1.15699 10 <sup>-4</sup>	2.77638 10 <sup>-5</sup>
<sup>11</sup> <sub>5</sub> B	1.40499 10 <sup>-4</sup>	1.26481 10 <sup>-4</sup>	1.68974 10 <sup>-5</sup>	3.59854 10 <sup>-4</sup>	5.27075 10 <sup>-4</sup>	1.26481 10 <sup>-4</sup>
Fe	0.6309028	0.6367991	0.6828925	0.5386364	0.4682990	0.6367991
Ni	0.0822917	0.0830607	0.0890729	0.0702569	0.0610825	0.0830607
Mn	0.0182870	0.0184579	0.0197940	0.0156126	0.0135739	0.0184579
Si	0.0091435	0.0092290	0.0098970	0.0078063	0.0067869	0.0092290
Cr	0.1737269	0.1753505	0.1880429	0.1483202	0.1289519	0.1753505

### 3.3.6 Homogenized water and zirconium region composition

The top and bottom regions of the fuel assemblies are smeared regions of the construction material, here assumed to be pure zirconium, and water. Table V shows the weight fractions of the borated water components and Zr. See Appendix A for the isotopic composition of Zr (in case separate isotopes of this element can be taken into account).

**Table V. Weight fraction per nuclide of smeared water and zirconium**

<b>component</b>	<b>bottom FA region</b>	<b>top FA region</b>
water density	0.74	0.66
water volume fraction	0.60	0.70
Zr volume fraction	0.40	0.20
void fraction	0.00	0.10
<b>Av. Density (g/cm<sup>3</sup>)</b>	<b>3.044</b>	<b>1.762</b>
<b>nuclide</b>	<b>weight fraction</b>	
<sup>1</sup> <sub>1</sub> H	0.0162913	0.0292856
<sup>16</sup> <sub>8</sub> O	0.1292776	0.2323919
<sup>10</sup> <sub>5</sub> B	5.25228 10 <sup>-5</sup>	9.44159 10 <sup>-5</sup>
<sup>11</sup> <sub>5</sub> B	2.39272 10 <sup>-4</sup>	4.30120 10 <sup>-4</sup>
Zr	0.8541393	0.7377980

### 3.4 Temperatures

The different temperatures in an operating reactor generally complicate the preparation of the cross sections, which can be strong functions of temperature. As the aim of this benchmark is not to calculate physical quantities of an operating reactor it was decided to take all cross sections (but not densities) in all materials at room temperature. This will not affect the simulation time of the neutron histories with table lookup of the cross sections (except when the cross sections are Doppler broadened to the required temperature at the moment they are needed in the simulation).

### 3.5 Cross sections

As in most current general-purpose Monte Carlo codes the energy dependence of the cross sections is treated in pseudo-continuous energy (pointwise) mode, this is the preferred option for this benchmark. There is no specification of the underlying evaluated nuclear data file. Therefore, cross sections normally available with the Monte Carlo code can be used. If no cross sections are available for the separate isotopes of a natural element (which may be the case for various construction materials) the composed cross section for the natural element can be used. As it will have an effect on the processing time of neutron histories, the thermal scattering in water (including all smeared regions with water) should be treated by the  $S(\alpha,\beta)$  thermal scattering law (at room temperature).

### 3.6 Fission energy

The actual calculation of the local fission power is in fact a complicated process as it is composed of different contributions. Due to the contribution of prompt and delayed photons, amongst others, part of the fission energy will not be deposited at the site where the fission event took place. For an extended discussion how these processes can be handled in a Monte Carlo calculation see Ref. 3. In the current benchmark we will consider neutron-only calculations assuming that all recoverable fission energy is deposited locally. In a later stage a more precise determination of the spatial distribution of the deposited fission energy can be considered.

## 4. Expected results

The aim of the benchmark test is to see whether a detailed calculation of local power densities can be made. The basic volume for the calculation of the power density is an axial region of a fuel pin of 1/100th of the fuel length, which is 3.66 cm. Hence, the expected results are the power densities expressed in  $W/cm^3$  per source neutron in all axial regions of all fuel pins and their standard deviation. As this constitutes a huge number of data, we selected a small number of regions to actually compare results. However, as the calculation of power densities in all regions seriously influences the calculation time, the final aim is to include the tallies for the power density of all axial regions of all fuel pins. As there are  $17 \times 17 \times 25 = 264$  fuel pins in an assembly and 241 assemblies, there are  $264 \times 241 \times 100 = 6,362,400$  power densities to be calculated. This may be too much for a computer system to accommodate in memory and to do in a reasonable computing time. *Therefore, if it is not possible to include tallies for all axial regions of all fuel pins, one should include all axial regions for as many fuel pins as possible in a fuel assembly for as many fuel assemblies as possible.*

To compare the power densities and their standard deviation for a selected number of regions we identify the fuel assemblies by two numbers indicating their position relative to the central fuel assembly, which is identified as (0,0). Also the fuel pins in an assembly are identified relative to the center pin in the assembly. The axial fuel regions are numbered from 1 at the bottom of the fuel pin to 100 at the top.

The following results should be reported.

1. The name of the participant(s)
2. Affiliation and e-mail address
3. The name of the Monte Carlo code and version number used for the calculation and a citable reference
4. The compiler used to create the Monte Carlo executable and any optimization options
5. The type of computer system used (operating system; processor type; single processor or parallel calculation; in the latter case also the number of nodes and/or cores used, and parallel software)
6. The nominal number of neutron histories per cycle (or batch or generation)
7. The number of inactive cycles (batches) to arrive at a converged source distribution
8. Qualitative description of the source distribution for the first cycle (batch)
9. The number of active cycles (batches)

10. The cumulative number of *actual* neutron histories during the active cycles (if available)
11. The execution time (min) for the active cycles in minutes (wall clock time and the reported CPU time when meaningful); if no separation in computing time between inactive and active cycles is available, quote the total execution time for all cycles
12. The actual number of separate fuel regions for which the power density is calculated (including all larger regions as discussed in task 14 and all regions for which the power density is calculated but not quoted as a result)
13.  $k_{eff}$  and its standard deviation (absolute value)
14. The total energy produced in the reactor core expressed in MeV per source neutron and its standard deviation (expressed as fraction of total energy)
15. The produced energy (expressed in MeV per source neutron) and their standard deviation (expressed as fraction of the energy) in the fuel regions specified in Table VI (notwithstanding the requirement to include all regions -or as many as possible- in the calculation).

**Table VI. Expected energy production for selected fuel regions**

<b>Result No</b>	<b>fuel assembly</b>	<b>fuel pin</b>	<b>axial region</b>	<b>comment</b>
15.1	(0, 0)	all, integrated	all, integrated	central FA
15.2	(3, 2)	all, integrated	all, integrated	
15.3	(-3, 2)	all, integrated	all, integrated	
15.4	(-3, -2)	all, integrated	all, integrated	
15.5	(3, -2)	all, integrated	all, integrated	
15.6	(-3, -8)	all, integrated	all, integrated	corner FA
15.7	(-6, 6)	all, integrated	all, integrated	corner FA
15.8	(6, 6)	all, integrated	all, integrated	corner FA
15.9	(3, 2)	(-8, -8)	all, integrated	pin at corner of FA
15.10	(3,2)	(2, 1)	all, integrated	
15.11	(3,2)	(2,1)	1	region at core bottom
15.12	(3,2)	(2,1)	50	region at core midplane
15.13	(3,2)	(2,1)	100	region at core top
15.14	(6,6)	(-8,-8)	100	

In Table VI “all, integrated” means that the fuel volume for which the produced energy is to be calculated is composed of all axial regions (i.e. over the full height of the fuel) in the specified fuel pin or in all fuel pins in the specified fuel assembly. As stated in Sect. 3.1 all fuel assemblies in the core should be modeled explicitly without assumptions on symmetry. Therefore, the energy produced in fuel assemblies or fuel pins or axial regions of fuel pins at symmetric positions in the core should be treated as separate tallies. In practice, due to depletion or specific design, symmetry may not exist and all tallies have to be taken into account.

16. Any other information relevant for the calculation; for instance modification to the original Monte Carlo code for this benchmark; special acceleration techniques or variance reduction techniques applied, improved estimation of variances, more detailed calculation of deposited fission energy, etc.
17. Optionally in case of a parallel execution of the calculation: the execution time when using less nodes and/or cores, for instance half the number of nodes or cores as in the reference calculation; if possible for several different numbers of nodes/cores. This will facilitate to extrapolate the execution time for many more nodes/cores than the reference calculation.

If tallies for all fuel regions could not be included in the calculation, two additional calculations are requested, with none and with about half (or some convenient fraction) the maximum number of tallies that were included for the main calculation in order to be able to extrapolate the computing time for the case with all required tallies. In this case the following additional results are expected.

18. The number of separate fuel regions for which the power density is calculated in the additional calculations.
19. The execution time (min) for the additional calculations

Finally, participants are encouraged to provide the input file used for the calculation for their specific Monte Carlo code.

## 5. Other remarks

It is known from the literature that there are still several issues in Monte Carlo criticality calculations for which no generally accepted solution exists today. The most important issues concern the convergence of the fission source distribution, especially for systems with high dominance ratio, the bias in  $k_{eff}$  and any other tally due to the correlation between successive cycles of fission neutrons and the underestimation of the variance and standard deviation of any tally estimate, also due to intercycle correlation [4]. Although these issues should be dealt with to obtain correct results, most general-purpose Monte Carlo criticality codes currently in use will not deal with them automatically. Therefore, it is up to the user to obtain a converged source distribution by using sufficient inactive cycles and to reduce the bias in tally results by using sufficient histories per cycle. The problem of underestimation of the standard deviation of a tally estimate cannot be solved by choosing appropriate input parameters for the Monte Carlo simulation. Therefore, in the current stage of the benchmark test, the “apparent” standard deviation, that is the standard deviation calculated according to the usual formula, is accepted.

Any attempts to get more reliable estimates of standard deviations would be appreciated. In a later stage, when generally accepted methods to deal with the above problems are found and included in Monte Carlo codes, these issues may also become a more explicit part of the benchmark test.

A first proposal of this benchmark was presented in Ref. 5. Here one can find some additional information about issues involved in this Monte Carlo performance benchmark. However, note that the specifications of the geometry and material composition have been changed, so actual results quoted in Ref. 5 do not apply to the current benchmark.

## **Acknowledgment**

We gratefully acknowledge the critical comments of Forrest Brown, Los Alamos National Laboratory, who also provided a streamlined version of the MCNP input file for the benchmark problem geometry.

## **References**

1. Kord Smith, "[Reactor Core Methods](#)," Invited lecture at the *M&C 2003 International Conference*, April 6-10, 2003, Gatlinburg, TN, USA (2003).
2. William R. Martin, "[Advances in Monte Carlo Methods for Global Reactor Analysis](#)," Invited lecture at the *M&C 2007 International Conference*, April 15-19, 2007, Monterey, CA, USA (2007).
3. Forrest Brown, William R. Martin, Russell D. Mosteller, "Monte Carlo – Advances and Challenges", Workshop at PHYSOR-2008, Interlaken, Switzerland, 14-19 September 2008, Report LA-UR-08-05891, Los Alamos National Laboratory (2009) [http://mcnp-green.lanl.gov/publication/mcnp\\_publications.html](http://mcnp-green.lanl.gov/publication/mcnp_publications.html).
4. Forrest Brown, "A Review of Monte Carlo Criticality Calculations – Convergence, Bias, Statistics", Proceedings M&C 2009, Saratoga Springs, NY, USA, May 3-7, 2009, on CD-ROM, American Nuclear Society, LaGrange Park, IL, USA (2009).
5. J. Eduard Hoogenboom and William R. Martin, "A Proposal for a Benchmark to Monitor the Performance of Detailed Monte Carlo Calculation of Power Densities in a Full Size Reactor Core", Proceedings M&C 2009, Saratoga Springs, NY, USA, May 3-7, 2009, on CD-ROM, American Nuclear Society, LaGrange Park, IL, USA (2009).

**Appendix A. Isotope fractions of some elements**

element	isotope	atom %	weight %
Boron	$^{10}_5\text{B}$	19.9	18.43
	$^{11}_5\text{B}$	80.1	81.57
Silicon	$^{58}_{28}\text{Si}$	92.223	91.866
	$^{60}_{28}\text{Si}$	4.685	4.834
	$^{61}_{28}\text{Si}$	3.092	3.300
Chromium	$^{50}_{24}\text{Cr}$	4.345	4.174
	$^{52}_{24}\text{Cr}$	83.789	83.699
	$^{53}_{24}\text{Cr}$	9.501	9.674
	$^{54}_{24}\text{Cr}$	2.365	2.453
Manganese	$^{55}_{25}\text{Mn}$	100	100
Iron	$^{54}_{26}\text{Fe}$	5.845	5.646
	$^{56}_{26}\text{Fe}$	91.754	91.901
	$^{57}_{26}\text{Fe}$	2.119	2.160
	$^{58}_{26}\text{Fe}$	0.282	0.293
Nickel	$^{58}_{28}\text{Ni}$	68.0769	67.198
	$^{60}_{28}\text{Ni}$	26.2231	26.776
	$^{61}_{28}\text{Ni}$	1.1399	1.183
	$^{62}_{28}\text{Ni}$	3.6345	3.835
	$^{64}_{28}\text{Ni}$	0.9256	1.008
Copper	$^{63}_{29}\text{Cu}$	69.15	68.48
	$^{65}_{29}\text{Cu}$	30.85	31.52
Zirconium	$^{90}_{40}\text{Zr}$	51.45	50.71
	$^{91}_{40}\text{Zr}$	11.22	11.18
	$^{92}_{40}\text{Zr}$	17.15	17.28
	$^{94}_{40}\text{Zr}$	17.38	17.89
	$^{96}_{40}\text{Zr}$	2.80	2.94
Molybdenum	$^{92}_{42}\text{Mo}$	14.77	14.15
	$^{94}_{42}\text{Mo}$	9.23	9.03
	$^{95}_{42}\text{Mo}$	15.90	15.73
	$^{96}_{42}\text{Mo}$	16.68	16.67
	$^{96}_{42}\text{Mo}$	9.56	9.66
	$^{98}_{42}\text{Mo}$	24.19	24.69
	$^{100}_{42}\text{Mo}$	9.67	10.07